



Pleistocene to Holocene phases of sedimentation and soil formation in the semiarid SE Spain (Eastern Betic Cordillera)

*Fases Pleistocenas y Holocenas de sedimentación aluvial y formación
de suelos en el SE semiárido de España (Cordilleras Béticas Orientales)*

Silva, P.G.⁽¹⁾; Roquero, E.⁽²⁾; Bardaji, T.⁽³⁾; Medialdea, A.⁽⁴⁾

(1) Dpto. Geología, Universidad de Salamanca, Escuela Politécnica Superior. Ávila Spain. pgsilva@usal.es

(2) Dpto. Edafología. E.T.S.I. Agrónomos. Universidad Politécnica de Madrid. Madrid, Spain. elvira.roquero@upm.es

(3) U.D. Geología. Universidad de Alcalá. Alcalá de Henares (Madrid), Spain. teresa.bardaji@uah.es

(4) Institute of Geography, Faculty Mathematics and Natural Sciences.

University of Cologne. Germany. amediald@uni-koeln.de

Abstract

This work uses the set of available regional geochronological data (OSL, TL, ^{14}C , Th/U) on alluvial sediments, calcretes and soils for the semiarid SE Spain to build a theoretical time-scale for the most important phases of sedimentation and soil formation occurred in the zone from the Middle Pleistocene to the Holocene. Most of the data come from the set of paleoseismic and paleoclimatic research carried out in the regions of Murcia and Almería over the past years. The gathered geochronological data set has 168 dates, 52 for calcic soils and calcretes and 116 for sediments and covers the last c. 400 ka. The analysis is based in the construction of age-frequency distribution functions discriminating bins of 5 ka, which offer enough resolution to distinguish among different Oxygen Isotopic Stages (OIS). The Holocene dataset is analysed separately discriminating time-bins of 0.5 ka according to the more robust data-set ^{14}C ages. Calcretes appears as elements developed during the last stages of warm isotopic stages (OIS 9 to 1), whilst sedimentation dominated during the transition between warm-cold isotopic stages, especially during terminations II to I, coinciding with deglaciation periods. During the Holocene the climatic events of 8.2 and 2.4 ka are clearly identified as drier periods with minor sedimentation, but enhanced calcrete formation, especially the first one.

Key words: Alluvial sedimentation; calcretes; chronology; Quaternary; Betic Cordillera; SE Spain.

Resumen

Este trabajo usa el conjunto de datos geocronológicos (OSL, TL, C^{14} , Th/U) sobre sedimentos aluviales, calcretas y suelos existentes para el SE semiárido de España con la finalidad de construir una escala temporal

teórica de las fases de sedimentación y formación de suelos más significativas ocurridas en la zona desde el Pleistoceno medio hasta el Holoceno. La mayoría de los datos proceden del conjunto de investigaciones paleoísmicas y paleoclimáticas realizadas en la zona de Murcia y Almería durante los últimos años. El conjunto de datos geocronológicos publicados recoge unas 168 fechas, 52 para suelos calizos y calcretas y 116 para sedimentos cubriendo los últimos c. 400 ka. El análisis se basa en la construcción de funciones de distribución de edad-frecuencia discriminando períodos de 5 ka, que ofrecen suficiente resolución para distinguir entre los diferentes estadios isotópicos de oxígeno (OIS) ocurridas durante el período de análisis. El conjunto de datos holocenos es analizado separadamente de acuerdo con el más robusto conjunto de edades C¹⁴ de que se dispone, permitiendo un análisis más detallado por periodos de 0,5 ka. Los resultados obtenidos indican que las calcretas son elementos que preferentemente se desarrollan durante las últimas etapas de los estadios isotópicos cálidos (OIS 9 al 1), mientras que la sedimentación es dominante durante la transición entre los estadios isotópicos fríos a cálido, especialmente durante las terminaciones II a I, coincidiendo con los períodos de deglaciación. Por su parte el análisis Holoceno identifica claramente los eventos de 8,2 y 2,4 ka como períodos más áridos con menor sedimentación, pero importantes picos en la formación de calcretas.

Palabras clave: Sedimentación aluvial; calcretas; cronología; Cuaternario; Cordillera Bética; SE España.

1. Introduction

The increasing development of dating techniques suitable for constructing fluvial chronologies has greatly expanded during the last few decades throughout Spain. Therefore, our understanding of how Mediterranean river systems respond to Quaternary climate change has improved from the early works of Lewin *et al.* (1995) and Macklin *et al.* (2002). These authors depicted a general pattern of sedimentation during cold periods and incision/floodplain stability during interglacial warm stages in the dryland river systems of the Mediterranean. However, more recent studies in the semiarid SE Spain indicate that calcretes are primarily warm stage elements and sedimentation is commonly attributed to increased sediment supply during glacial to interglacial transitions (cold to warm OIS; Schulte *et al.*, 2008; Silva *et al.*, 2008; Candy and Black, 2009; Roquero *et al.*, 2019a). These studies mainly come from the Murcia and Almería regions, however most of these works use limited geochronological datasets and their coverage is usually local.

At present there is a large dataset of age estimations for fine-grained alluvial sediments based in OSL/IRSL techniques, U/Th dating of calcrete horizons and calcic soils, but also

a large amount of ¹⁴C ages from organic materials contained in both soils and sediments in SE Spain (Eastern Betic Cordillera). Consequently, at this moment it is possible to manage the large geochronological dataset (OSL, IRSL, TL, Th/U, ¹⁴C) on alluvial sediments, calcretes and soils for the semiarid SE Spain to build a theoretical time-scale for the most important phases of sedimentation and soil formation occurred in the zone from the Middle Pleistocene to the present. Geochronological data from the last 400 ka mainly come from the increasing number of paleoseismic and paleoclimatic research in the regions of Murcia and Almería during the last years (i.e. Calmel-Avila, 2002; Masana *et al.*, 2004; 2005; Schulte *et al.*, 2008; Silva *et al.*, 2008; Candy and Black, 2009; Ortúñoz *et al.*, 2012; Insua *et al.*, 2015; Ferrater *et al.*, 2017; Masana *et al.*, 2018; Roquero *et al.*, 2019b; Fig. 1). Older age estimations (>400 ka) come from theoretical paleoclimatic analogues recently developed in the zone by the authors (Roquero *et al.*, 2019a) in paleosol sequences offset by the Palomares fault near Pulpí (Almería).

Of special interest is the paper by Candy and Black (2009), which developed “geochronological frequency distribution” functions to analyse phases of calcrete formation in

the Almería Region with a limited dataset of 24 Th/U age estimations. In the present paper we use a total of 168 age estimations to develop such age functions, 116 for alluvial sediments and 52 for calcic soils and calcretes to investigate the Quaternary timing of sedimentation and soil formation. From this large dataset about 75 dates correspond to the Holocene (c. last 11 ka). This Holocene dataset, mainly constituted by more accurate ^{14}C ages estimations (σ_1), allows a separate finer analysis to investigate relationships between climatic variations and its impact on prehistoric Neolithic, Chalcolithic and Bronze age populations in SE Spain based in the works of Calmel-Avila (2002) and Blanco *et al.* (2018).

2. Geologic background

The investigated area is located in the semi-arid SE Spain, within the Eastern Betic Cordillera (Fig. 1). This zone is the most tectonically active area of the Iberian Peninsula and record relevant landscape changes and basin inversion process during the Quaternary Period due to climatic but also tectonic forcings (Silva *et al.*, 2014; Harvey *et al.*, 2014). The Almería and Murcia regions record important paleogeographic changes during the last 3 Ma. Late Neogene marine basins were uplifted and begun their fluvial incision, but also new tectonic Quaternary basins were created (i.e. Guadalentín Depression) being the locus of new alluvial sedimentation (Harvey *et al.*, 2014; Silva *et al.*, 2014). In this context, large faulted mountain fronts emerged in the Almería and Murcia regions (Silva *et al.*, 2003) feeding relevant alluvial fan systems which were the main morphosedimentary systems in the zone throughout the Quaternary (Harvey *et al.*, 2014). Despite lithological controls in the drainage basins, tectonics (firstly) and climate (secondly) controlled alluvial fan development in SE Spain (Silva *et al.*, 2014).

Fan development in SE Spain is characterized by three broad phases of sedimentation (Silva *et al.*, 1992) supporting differentially deve-

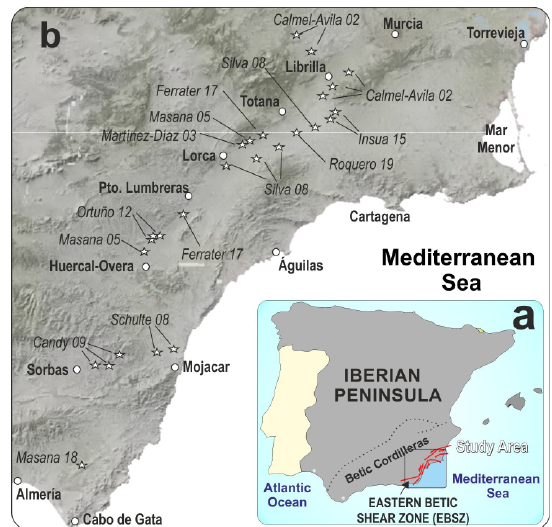


Figure 1. Location of the more relevant outcrops for the age data sets used in this study. (a) Location within the Iberian Peninsula; (b) Location in SE Spain. The stars indicate the papers (first author and year of publication) in which the age data sets appeared.

Figura 1. Localización de los afloramientos más importantes de donde proceden el conjunto de dataciones utilizadas en el presente estudio. (a) Localización de la zona de estudio en la Península Ibérica. (b) Localización de los afloramientos en el SE de España. Las estrellas indican los trabajos (primer autor y año de publicación) en los que se describen las diferentes dataciones.

loped mature to young calcretes at their respective surfaces (Alonso-Zarza *et al.*, 1998; Silva, 2014). Geochronological data for the area allowed to precise that older preserved alluvial fan surfaces in the Guadalentín Depression belong to the late Middle Pleistocene (Silva, 2014) with top sediments and calcretes dated (OSL and Th/U respectively) around the Oxygen Isotopic Stage OIS 9 (c. 300 ka; Candy and Black, 2009; Ortuño *et al.*, 2012; Roquero *et al.*, 2019a), which are present in the preserved surfaces of the first depositional phase of Silva *et al.* (1992). Data from Candy and Black (2009) indicate that calcrete development has peaks of intense formation during the following warm isotopic stages OIS 5 and OIS 1. Geochronological data indicate that during the warm stages OIS7 and OIS 3 calcrete development was not a dominant process in the area. On the contrary, the last interglacial (OIS 5) and the present inter-

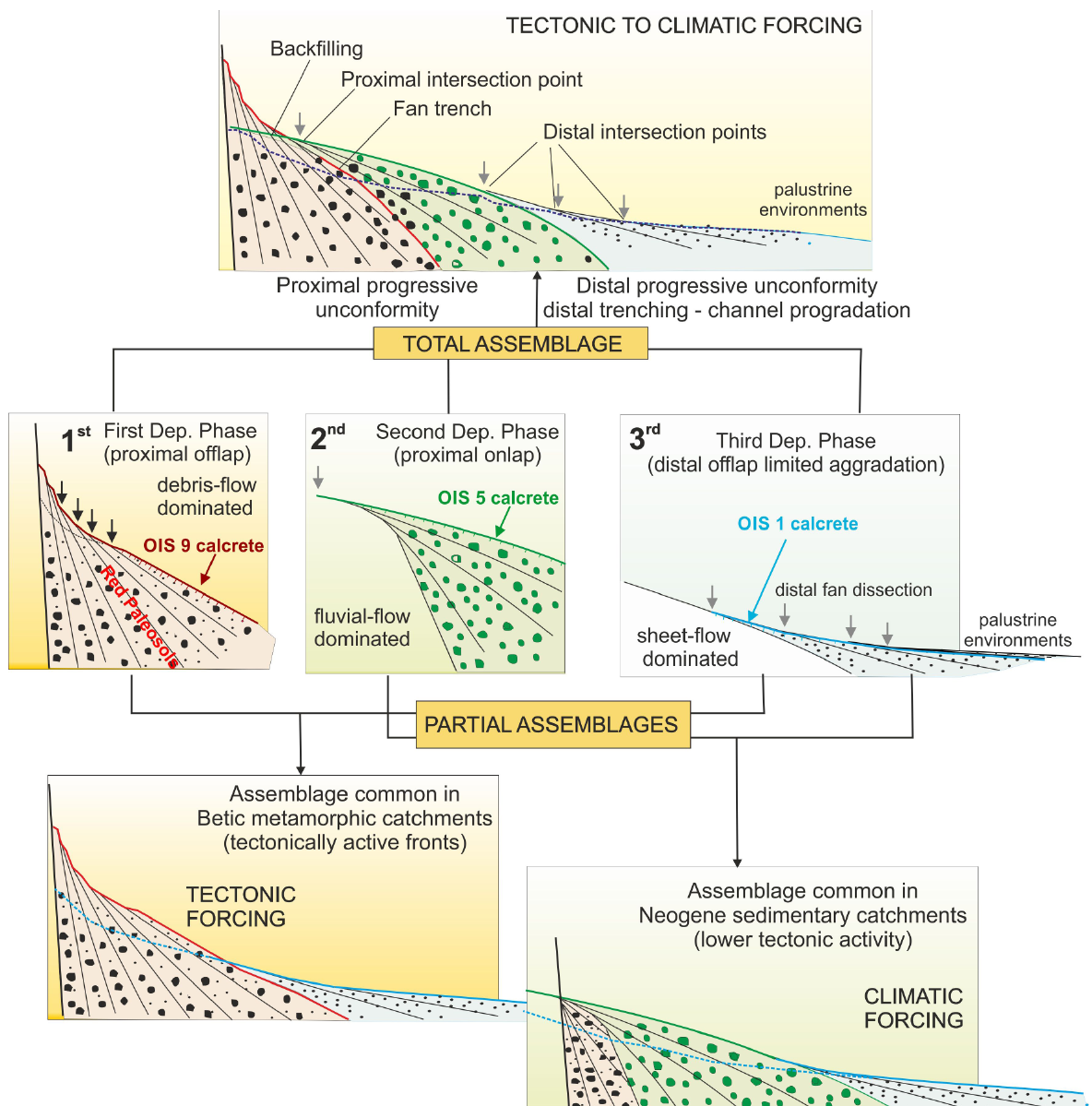


Figure 2. Assemblage and characteristics of alluvial fan bodies along the margins of the Guadalentín Depression illustrating tectonic and climatic forcing from the Middle Pleistocene to the Holocene during the sedimentation of the three main depositional sequences identified in the zone. (modified from Silva, 2014).

Figura 2. Ensamblaje geomorfológico y características de los abanicos aluviales a lo largo de los márgenes de la Depresión del Guadalentín ilustrando los controles tectónicos y climáticos sobre los mismos desde el Pleistoceno Medio al Holoceno durante las tres fases de sedimentación aluvial identificadas en la zona (modificado de Silva, 2014).

glacial (OIS 1) are the culminating periods for the second and third phases of alluvial fan development in the zone (Silva, 2014). The second depositional phase of fan development was controlled by proximal offlap and backfilling, indicating the end of significant

tectonic forcing on fan development and generating large stable surfaces for calcrete development during the OIS5 (Fig. 2). This second episode of calcrete formation overprinted the already crusted surfaces of the first depositional phase of alluvial fans, but

also contributed in different pulses to the re-carbonation of previous red paleosols. This last process was however active soon before the development of the OIS 9 calcrete, according to the progressive aridification of the zone during the last 500 ka (Fig. 3; Roquero *et al.*, 2019a). The younger phase of alluvial sedimentation is featured by fanhead trench development in the fan surfaces of the previous phases, limited distal aggradation and generation of intersection point scours. Consequently, this scenario promoted the distal dissection of the fan systems (Fig. 2) favouring the integration of fan channels in the regional fluvial network during the early Holocene ("Down-fan erosion" or "Downward erosion" *sensu* Silva, 2014).

During the late Holocene, several prehistoric and historic (Chalcolithic, Bronze age, Roman Period and Little Ice age) sedimentation pulses occurs within the Guadalentín Depression with intervening phases of soil development (Calmel-Avila, 2002; Silva *et al.*, 2008). All these ultimate sedimentary inputs are

related to very limited distal aggradation in the alluvial fan systems, but also to the first stages of fluvial dissection of the previous endorheic areas (palustrine zones) from the Late Chalcolithic Period (c. 2.800 BP; Silva *et al.*, 2008). Fluvial dissection was truly effective in the area from the Bronze Age (c. 2.400 BP), triggering the nearly desiccation of the ancient wetlands and the virtual depopulation of the area (Calmel-Avila, 2002). Older Quaternary fan surfaces are preserved in the Campo de Cartagena – Mar Menor Basin at Murcia (Somoza *et al.*, 1989) or in the Níjar-Campo Dalías Basin at Almería (Goy and Zazo, 1984). These old surfaces support very thick salmon-coloured calcrete profiles (i.e. Montenat, 1978) consequence of the carbonation, re-digestion and cementation of previous Mediterranean red soils developed during more humid conditions (Silva, 2014; Roquero *et al.*, 2019a). The existing paleomagnetic data indicate that former red soils developed from about the Brunhes-Matuyama reversal c. 780 ka (Somoza *et al.*, 1989) during the first depositional phase of

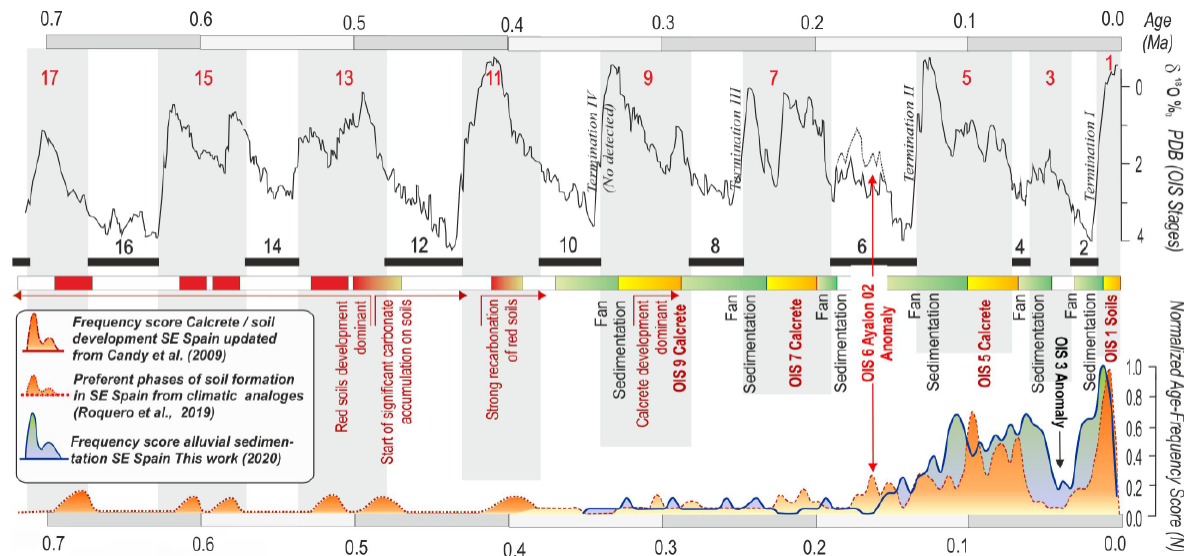


Figure 3. Normalized frequency distribution curve for sediment (solid line) and soil calcrete (dotted line) scores for the last c. 700 ka calculated in this study. The upper graph represents the conventional global OIS curve in function of the $\delta^{18}\text{O}$ values from oceanic records. Climatic framework modified from Roquero *et al.* (2019).

Figura 3. Curva de distribución de frecuencias normalizadas para los scores acumulados de sedimentos (línea continua) y suelos calcáreos (líneas discontinuas) para los últimos c. 700 ka obtenidos en este estudio. El gráfico superior representa la curva OIS global convencional en función de los valores de $\delta^{18}\text{O}$ de los registros oceánicos. Marco climático modificado de Roquero *et al.* (2019).

alluvial fan development (Roquero *et al.*, 2019a). Consequently, there are no data for previous phases of alluvial sedimentation, since these sediments were tectonically incorporated to the reliefs (Fig. 2) and/or the dominant sedimentation in the present inland areas was shallow marine or littoral at those times (Silva *et al.*, 2014).

To the south (Almería region), alluvial fan sedimentation was also dominant during most of the lower and Middle Pleistocene (Goy and Zazo, 1986; García-Meléndez *et al.*, 2003; Stokes *et al.*, 2008; 2019), but river incision occurred from the Middle Pleistocene. This is the case of the Almanzora and Aguas-Feos river valleys, two of the most studied fluvial systems in the Almería region (i.e. Harvey *et al.*, 1995; Wezens and Wezens, 1997; Stokes *et al.*, 2008; Schülte *et al.*, 2008; Candy and Black, 2009). Calcretes developed in individual terrace surfaces indicate that the older calcrete with an age of 309 ± 26 ka (i.e. OIS 9) corresponds to the terrace at c. +50m above the present thalweg of the Aguas valley (Candy and Black, 2009). $^{10}\text{Be}/^{26}\text{Al}$ cosmogenic dating of the Aguas river terraces around the locality of Sorbas indicate that river incision occurred from at least 1.0 - 0.8 Ma, but accelerated in this area from the end of the Mid Pleistocene Transition (MPT) around c. 400 - 500 ka, due to climatic and tectonic forcings (Illiot, 2014; Stokes *et al.*, 2018).

From the existing literature, it seems clear that the transition from littoral to terrestrial environments, as well as the progress from alluvial sedimentation to fluvial dissection, advanced from south to north across the whole Eastern Betic Cordillera. This northward progression indicates an advance of uplift in the same direction throughout the Quaternary, allowing a prevalence of shallow marine and littoral environments to the north (Murcia) well into the late Pleistocene and even into the Holocene (Silva *et al.*, 2014; Harvey *et al.*, 2014). In the northern zones of Murcia fluvial incision were not totally effective until the Late Bronze Age around 2.0 - 2.4 ka BP (Calmel-Avila, 2002), and littoral estuarine

and lagoonal environments prevailed until the Middle Ages in the Lower Segura Depression (Silva *et al.*, 2015).

3. Methodology

3.1. The Quaternary dataset

In order to create the more robust possible database on calcrete (soil) development and alluvial sedimentation for the region we have collected all the available geochronological data coming from paleoclimatic and fault trenching studies in the zone published to the date. We have included the calcrete Th/U age dataset from Candy and Black (2009) complemented with other Th/U age estimations from Masana *et al.* (2005), Ferrater *et al.* (2017) and Masana *et al.* (2018), completing a total of 37 age-estimations (Table 1) for the studied period. TL, OSL, IRSL and ^{14}C age data for sediments complete a total of 56 dates from a large variety of research published for the zone (see Tables 2a and 2b). The compiled dataset for this period (93 ages) has been analysed by means of a “geochronological frequency distribution” like that used by Candy *et al.* (2009). This analysis considers not just the mean ages themselves resulting of the different dating methods, but the uncertainties associated with each age estimate (\pm Errors). This is of significance here, since we are comparing ages resulting from diverse analytical methods with different dating precision. The collected Quaternary database of ages and related uncertainties cover the last c. 400 ka for both calcretes and sediments (Tables 1 and 2), which is imposed by the common age-limits of the used analytical methods.

The calcrete dataset is basically the same than those used by Candy and Black (2009) with few complementary Th/U age existing for the zone. The older calcrete age data is 304 ± 24 ka and the younger one 6.6 ± 9.2 ka (Table 1). The alluvial sediment dataset is newly analysed in this study and the older age is 324 ± 24 ka. In this dataset, ages younger than 5.0 ka have been excluded since they come from fault-trenching analyses and these ages

Table 1. Details on ages of calcretes provided by different authors for Holocene and Pleistocene deposits in the semi-arid SE Spain (Almería and Murcia regions) using different methods of Th/U dating. Age estimations for late Holocene soils (< 5.5 ka) in Table 3.

Tabla 1. Detalles de las dataciones en calcretas recogidas por diferentes autores para los depósitos del Holoceno y Pleistoceno en el SE Semiárido de España (regiones de Murcia y Almería) mediante su datación por diferentes métodos Th/U. Las dataciones para los suelos carbonatados del Holoceno reciente (< 5,5 ka) se encuentran listadas en la tabla 3.

Rank	Zone	Landform	Authors (year)	Dating Method	Age	Error-	Error+	OIS
1	Sorbas	Terrace	Candy <i>et al.</i> , 2009	Th/U Alpha	6.60	0.92	0.92	OIS 1
2	Sorbas	Terrace	Candy <i>et al.</i> , 2009	Th/U Alpha	7.90	4.70	4.70	OIS 1
3	Sorbas	Terrace	Candy <i>et al.</i> , 2009	Th/U Alpha	8.00	0.00	2.70	OIS 1
4	Sorbas	Terrace	Candy <i>et al.</i> , 2009	Th/U Alpha	8.97	0.28	0.28	OIS 1
5	Sorbas	Terrace	Candy <i>et al.</i> , 2009	U/Th Tims	9.02	0.71	0.71	OIS 1
6	Sorbas	Terrace	Candy <i>et al.</i> , 2010	U/Th Tims	9.67	0.82	0.82	OIS 1
7	Lorca	Fan	Ferrater <i>et al.</i> , 2017	Th/U Alpha	11.0	1.70	1.70	OIS 1
8	Lorca	Fan	Ferrater <i>et al.</i> , 2017	Th/U Alpha	11.7	2.60	2.60	OIS 1
9	Lorca	Fan	Ferrater <i>et al.</i> , 2017	Th/U Alpha	12.39	0.42	0.42	OIS 2
10	Sorbas	Terrace	Candy <i>et al.</i> , 2009	U/Th Tims	12.14	0.37	0.37	OIS 2
11	Carboneras	Fan	Masana <i>et al.</i> , 2018	Th/U Alpha	13.70	6.50	6.80	OIS 2
12	Sorbas	Terrace	Candy <i>et al.</i> , 2009	Th/U Alpha	14.00	20.00	20.00	OIS 2
13	Carboneras	Fan	Masana <i>et al.</i> , 2018	Th/U Alpha	18.00	10.20	11.30	OIS2
14	Carboneras	Fan	Masana <i>et al.</i> , 2018	Th/U Alpha	19.40	14.10	16.00	OIS2
15	Lorca	Fan	Ferrater <i>et al.</i> , 2017	Th/U Alpha	20.90	2.50	2.50	OIS 2
16	Goñar	Fan	Ferrater <i>et al.</i> , 2017	Th/U Alpha	23.20	4.20	4.20	OIS 2
17	Goñar	Fan	Ferrater <i>et al.</i> , 2017	Th/U Alpha	46.60	5.70	5.70	OIS3
18	Lorca	Fan	Masana <i>et al.</i> , 2005	Th/U Alpha	65.19	2.20	2.25	OIS 3
19	Sorbas	Terrace	Candy <i>et al.</i> , 2009	U/Th Tims	69.80	4.70	4.70	OIS 4
20	Sorbas	Terrace	Candy <i>et al.</i> , 2009	U/Th Tims	68.00	32.00	32.00	OIS 4
21	Sorbas	Terrace	Candy <i>et al.</i> , 2009	U/Th Tims	77.10	4.40	4.40	OIS 5
22	Sorbas	Terrace	Candy <i>et al.</i> , 2009	U/Th Tims	77.70	4.40	4.40	OIS 5
23	Sorbas	Terrace	Candy <i>et al.</i> , 2009	Th/U Alpha	80.00	19.00	19.00	OIS 5
24	Sorbas	Terrace	Candy <i>et al.</i> , 2009	Th/U Alpha	91.00	11.00	11.00	OIS 5
25	Sorbas	Terrace	Candy <i>et al.</i> , 2009	Th/U Alpha	92.00	41.00	41.00	OIS 5
26	Sorbas	Terrace	Candy <i>et al.</i> , 2009	Th/U Alpha	98.00	30.00	30.00	OIS 5
27	Sorbas	Terrace	Candy <i>et al.</i> , 2009	Th/U Alpha	103.00	33.00	33.00	OIS 5
28	Goñar	Fan	Ferrater <i>et al.</i> , 2017	Th/U Alpha	105.10	4.20	4.20	OIS 5
29	Sorbas	Terrace	Candy <i>et al.</i> , 2009	U/Th Tims	112.00	15.00	15.00	OIS 5
30	Carboneras	Fan	Masana <i>et al.</i> , 2018	Th/U Alpha	132.70	5.90	6.20	OIS 5
31	Sorbas	Terrace	Candy <i>et al.</i> , 2009	Th/U Alpha	147.00	25.00	25.00	OIS 6
32	Sorbas	Terrace	Candy <i>et al.</i> , 2009	U/Th Tims	155.00	9.00	9.00	OIS 6
33	Carboneras	Fan	Masana <i>et al.</i> , 2018	Th/U Alpha	162.30	1190	11.00	OIS 5
34	Sorbas	Terrace	Candy <i>et al.</i> , 2009	U/Th Tims	207.00	11.00	11.00	OIS 7
35	Sorbas	Terrace	Candy <i>et al.</i> , 2009	Th/U Alpha	224.00	160.00	160.00	OIS 7
36	Sorbas	Terrace	Candy <i>et al.</i> , 2009	U/Th Tims	304.00	26.00	26.00	OIS 9
37	Sorbas	Terrace	Candy <i>et al.</i> , 2009	Th/U Alpha	>350.00			≥ OIS 9

Table 2a. Details on available published ages of Pleistocene alluvial deposits (OIS2 – OIS 4) provided by several authors in the semi-arid SE Spain (Almería and Murcia region) using different dating methods: Radiocarbon (^{14}C); Quartz Thermoluminiscence (TL); Quartz optically stimulated luminescence (OSL); K-feldspar post-infrared stimulated luminescence (IRSL - pirIR), see also Shobati et al. (2011). Age estimations for older Pleistocene deposits ($\geq \text{OIS } 5$) in table 2b. Age estimations for Holocene (OIS 1) sediments in table 4.

Tabla 2a. Detalles sobre las edades publicadas para depósitos aluviales pleistocenos (OIS2 – OIS 4) proveídas por diferentes autores para el SE semiárido de España (regiones de Murcia y Almería) mediante su datación por diferentes métodos: Carbono catorce (^{14}C); termoluminiscencia convencional (TL); Termoluminiscencia ópticamente estimulada (OSL); Termoluminiscencia estimulada post-infrarroja (IRSL - pirIR). Consultar también Shobati et al. (2011). Edades para depósitos más antiguos ($\geq \text{OIS } 5$) en la tabla 2b. Edades para los depósitos holocenos en tablas 4a y 4b.

Rank	Zone	Landform	Authors (year)	Dating Method	Age	Error-	Error+	OIS
1	Goñar	Fan	Ortuño et al. (2012)	IRSL	14.00	2.00	2.00	OIS 2
2	Lorca	Fan	Martínez Díaz et al. (2003)	TL	14.50	1.70	1.70	OIS 2
3	Lorca	Fan	Masana et al. (2004)	TL	14.90	1.60	1.60	OIS 2
4	Lorca	Fan	Masana et al. (2004)	^{14}C	15.94	0.05	0.05	OIS 2
5	Lorca	Fan	Martínez Díaz et al. (2003)	TL	17.20	2.10	2.10	OIS 2
6	Lorca	Fan	Masana et al. (2004)	TL	17.20	2.10	2.10	OIS 2
7	Lorca	Fan	Masana et al. (2004)	TL	17.20	2.30	2.30	OIS 2
8	Lorca	Fan	Masana et al. (2004)	TL	17.80	2.00	2.00	OIS 2
9	Lorca	Fan	Martínez Díaz et al. (2003)	TL	22.20	3.20	3.20	OIS 2
10	Goñar	Fan	Ortuño et al. (2012)	IRSL	23.00	2.00	2.00	OIS 2
11	Lorca	Fan	Masana et al. (2004)	TL	23.10	3.00	3.00	OIS 2
12	Lorca	Fan	Martínez Díaz et al. (2003)	TL	23.80	3.10	3.10	OIS 2
13	Lorca	Fan	Martínez Díaz et al. (2003)	TL	25.40	3.10	3.10	OIS 2
14	Lorca	Fan	Masana et al. (2004)	TL	27.00	3.80	3.80	OIS 2
15	Carboneras	Fan	Masana et al. (2018)	TL	28.7	1.80	2.10	OIS3
16	Huércal	Fan	Masana et al. (2005)	TL	34.20	3.50	4.10	OIS 2
17	Carboneras	Fan	Masana et al. (2018)	^{14}C	41.65	0.85	0.85	OIS3
19	Goñar	Fan	Ortuño et al. (2012)	OSL	43.70	5.00	6.00	OIS 3
20	Goñar	Fan	Ortuño et al. (2012)	OSL	46.30	5.10	6.10	OIS 3
21	Goñar	Fan	Ortuño et al. (2012)	IRSL	49.00	2.00	2.00	OIS 3
22	Goñar	Fan	Ortuño et al. (2012)	OSL	52.40	6.40	7.90	OIS 4
23	Huércal	Fan	Masana et al. (2005)	TL	53.90	7.50	9.40	OIS 4
24	Huércal	Fan	Masana et al. (2005)	TL	56.80	5.00	6.30	OIS 4
25	Goñar	Fan	Ortuño et al. (2012)	IRSL	58.00	3.00	3.00	OIS 4
26	Goñar	Fan	Ortuño et al. (2012)	IRSL	61.00	2.00	2.00	OIS 4
27	Goñar	Fan	Ortuño et al. (2012)	OSL	61.90	11.20	15.00	OIS 4
28	Huércal	Fan	Masana et al. (2005)	TL	63.20	8.90	11.60	OIS 4
29	Huércal	Fan	Masana et al. (2005)	TL	68.60	9.40	12.60	OIS 4
30	Carboneras	Fan	Masana et al. (2018)	TL	69.80	9.80	13.20	OIS4
31	Carboneras	Fan	Masana et al. (2018)	TL	70.2.	10.50	14.40	OIS4

Table 2b (continuation). Details on available published ages of Pleistocene alluvial deposits (\geq OIS 5) provided by several authors in the semi-arid SE Spain (Almería and Murcia region) using different dating methods: Quartz Thermoluminescence (TL); Quartz optically stimulated luminescence (OSL); K-feldspar post-infrared stimulated luminescence (IRSL - pIRIR), see also Shobati *et al.* (2011).

Tabla 2b (continuación). Detalles sobre las edades publicadas para depósitos aluviales pleistocenos (\geq OIS 5) proveídas por diferentes autores para el SE semiárido de España (regiones de Murcia y Almería) mediante su datación por diferentes métodos: Termoluminiscencia convencional (TL); Termoluminiscencia ópticamente estimulada (OSL); Termoluminiscencia estimulada post-infrarroja (IRSL - pIRIR). Consultar también Shobati et al. (2011).

Rank	Zone	Landform	Authors (year)	Dating Method	Age	Error-	Error+	OIS
32	Carboneras	Fan	Masana <i>et al.</i> (2018)	TL	73.10	13.60	19.40	OIS5
33	Carboneras	Fan	Masana <i>et al.</i> (2018)	TL	79.40	11.70	16.6	OIS5
34	Carboneras	Fan	Masana <i>et al.</i> (2018)	TL	83.30	14.20	21.00	OIS5
35	Carboneras	Fan	Masana <i>et al.</i> (2018)	TL	87.70	14.70	22.10	OIS5
36	Carboneras	Fan	Masana <i>et al.</i> (2018)	TL	87.90	14.80	22.40	OIS5
37	Carboneras	Fan	Masana <i>et al.</i> (2018)	TL	89.30	14.70	22.20	OIS5
38	Huércal	Fan	Masana <i>et al.</i> (2005)	TL	94.00	14.00	21.00	OIS 5
39	Huércal	Fan	Masana <i>et al.</i> (2005)	TL	104.00	18.00	29.00	OIS 5
40	Carboneras	Fan	Masana <i>et al.</i> (2018)	TL	106.00	17.00	27.20	OIS5
41	Goñar	Fan	Ortuño <i>et al.</i> (2012)	IRSL	107.00	5.00	5.00	OIS 5
42	Goñar	Fan	Ortuño <i>et al.</i> (2012)	IRSL	108.00	8.00	8.00	OIS 5
43	Goñar	Fan	Ortuño <i>et al.</i> (2012)	OSL	111.00	21.00	36.00	OIS 5
45	Goñar	Fan	Ortuño <i>et al.</i> (2012)	OSL	120.00	21.00	39.00	OIS 5
46	Huércal	Fan	Masana <i>et al.</i> (2005)	TL	121.00	20.00	0.00	OIS 5
47	Goñar	Fan	Ortuño <i>et al.</i> (2012)	OSL	126.00	23.00	0.00	OIS 5
48	Goñar	Fan	Ortuño <i>et al.</i> (2012)	IRSL	131.00	6.00	6.00	OIS 6
49	Goñar	Fan	Ortuño <i>et al.</i> (2012)	IRSL	142.00	7.00	7.00	OIS 6
50	Goñar	Fan	Ortuño <i>et al.</i> (2012)	IRSL	152.00	7.00	7.00	OIS 6
51	Goñar	Fan	Ortuño <i>et al.</i> (2012)	IRSL	191.00	17.00	17.00	OIS 6
52	Goñar	Fan	Ortuño <i>et al.</i> (2012)	IRSL	235.00	10.00	10.00	OIS 8
53	Goñar	Fan	Ortuño <i>et al.</i> (2012)	IRSL	258.00	16.00	16.00	OIS 8
54	Goñar	Fan	Ortuño <i>et al.</i> (2012)	IRSL	290.00	13.00	13.00	OIS 8
55	Goñar	Fan	Ortuño <i>et al.</i> (2012)	IRSL	324.00	24.00	24.00	OIS 8

are the most numerous (75 over the total 168 ages used in this study) and would generate artificial peaks during the Late Holocene. Accordingly, the Holocene data set (last c. 11.7 ka) has been subject of a separate more detailed analysis (see section 3.2). For the Quaternary dataset, ages with oversized uncertainty ranges over ± 50 ka were also excluded, since they can overlap several isotopic stages, especially those occurred after OIS6. This is the case of some age data published by Candy *et al.* (2009) and Schütte *et al.* (2008). Finally,

existing ages from travertine deposits in the zone (i.e. Schütte *et al.*, 2008; Delgado Castilla, 2009) were not used, since these carbonate bodies are difficult to assign to phases of sedimentation or soil formation.

Following the method proposed by Candy and Black (2009), the time-span covered by the geochronological dataset has been subdivided into time-bins of 5000 years (5 ka) and the occurrence of ages and uncertainties in each of the bins is weighted through a

score attached to the mean age itself (value =3) and the time-span covered by its associated uncertainty (value=1). For instance, a bin that contains one mean age (value =3) and is overlapped by an uncertainty of other sample (value =1) would receive a score of 4, whilst a bin that contains two mean ages (value: 3 + 3 =6) and overlapped by two uncertainties (value: 1 + 1 =2) would receive a score of 8 (Candy and Black, 2009; page 10).

Due to the misbalance between the number of age-data for soils and sediments (37 vs 56), as well as for maximum and minimum individual and total values of their respective scores (410 sediment vs 266 soil data) both datasets were normalized in order to provide a weighted comparison. Normalization is a statistical operation commonly used in morphometric analyses and digital map algebra in order to scale numeric or spatial datasets for their comparison (i.e. river log-profiles). This operation converts numeric datasets in values between 1 (100%: maximum) and 0 (0%: minimum) leading their comparison or computation by algebra functions. The resulting frequency dis-

tribution for SE Spain (Murcia-Almería regions) is shown in figure 3, which display peaks and lows of sediment/soil production in relation to the conventional climatic scale of OIS stages resulting from oceanic records.

3.2. The Holocene dataset

The gathered geochronological dataset for the last 11.000 years completes about 75 dates, 15 of which correspond to calcretes and calcic soils (Table 3) and the rest 60 age-estimations to sediments, most of them ^{14}C data (Tables 4a and 4b). The applied method is also based on the “geochronological frequency distribution” of Candy and Black, (2019) used for the Quaternary dataset in the previous section functions. In this case, the wider and robust number of ^{14}C data existing in the zone allows to construct more detailed age-frequency functions discriminating periods (bins) of only 500 years (0.5 ka). The occurrence of ages and uncertainties in each of the bins is weighted through a score (value = 3). This score considers the mean age

Table 3. Details on ages of calcretes and pedogenic carbonates provided by different authors for Holocene soils in the semi-arid SE Spain (Almería and Murcia regions) using different methods: Radiocarbon (^{14}C); Series Th/U.

Tabla 3. Detalles sobre dataciones en calcretas y carbonato endofogénico publicadas por diferentes autores para suelos del Holoceno en el SE semiárido de la Península Ibérica (regiones de Murcia y Almería) mediante su datación por diferentes métodos: Carbono catorce (^{14}C); Th/U series.

Rank	Zone	Landform	Soil	Authors (year)	Dating Method	Age	Error ±
1	Librilla, MU	Fan	Pedogenic	Calmel-Avila, 2000	^{14}C	2.51	0.05
2	Totana, MU	Fan	Pedogenic	Silva <i>et al.</i> , 2008	^{14}C	2.72	0.04
3	Alfaix, AL	Terrace	Pedogenic	Schulte <i>et al.</i> , 2008	^{14}C	4.01	0.08
4	Lorca, MU	Fan	Cinder level	Strydonck <i>et al.</i> , 1995	^{14}C	4.10	0.04
5	Alfaix, AL	Terrace	Pedogenic	Schulte <i>et al.</i> , 2008	^{14}C	5.39	0.08
6	Sorbas, AL	Terrace	Nodular calc.	Candy <i>et al.</i> , 2009	Th/U Alpha	6.60	0.92
7	Sorbas, AL	Terrace	Nodular calc.	Candy <i>et al.</i> , 2009	Th/U Alpha	7.90	4.70
8	Sorbas, AL	Terrace	Nodular calc.	Candy <i>et al.</i> , 2009	Th/U Alpha	8.00	2.60
9	Sorbas, AL	Terrace	Nodular Calc.	Candy <i>et al.</i> , 2009	Th/U Alpha	8.97	0.28
10	Sorbas, AL	Terrace	Nodular Calc.	Candy <i>et al.</i> , 2009	U/Th Tims	9.02	0.71
11	Sorbas, AL	Terrace	Nodular Calc.	Candy <i>et al.</i> , 2010	U/Th Tims	9.67	0.82
12	Lorca, MU	Fan	Nodular Calc.	Ferrater <i>et al.</i> , 2017	Th/U Alpha	11.0	1.70
13	Lorca, MU	Fan	Massive Calc.	Ferrater <i>et al.</i> , 2017	Th/U Alpha	11.7	2.60

Table 4a. Details on available published ages of late Holocene alluvial deposits (OIS1) provided by several authors in the semiarid SE Spain (Almería and Murcia region) using different dating methods: Radiocarbon (^{14}C); Quartz Thermoluminescence (TL); Quartz optically stimulated luminescence (OSL).

Tabla 4a. Detalles sobre las edades publicadas para depósitos aluviales del Holoceno reciente proporcionadas por diferentes autores para el SE semiárido de España (regiones de Murcia y Almería) mediante su datación por diferentes métodos: Carbono catorce (^{14}C); Termoluminiscencia convencional (TL); Termoluminiscencia ópticamente estimulada (OSL).

Rank	Zone	Site	Landform	Authors (year)	Dating Method	Age	Error ±	bin
1	Totana, MU	Río (Guad)	Lacustrine	Insua <i>et al.</i> (2015)	^{14}C	0.19	0.03	
2	Lorca, MU	Colmenar	Fan Terrace	Martínez Díaz <i>et al.</i> (2003)	^{14}C	0.34	0.04	500 – 0
3	Lorca, MU	Colmenar	Fan Terrace	Martínez Díaz <i>et al.</i> (2003)	^{14}C	0.48	0.04	
4	Librilla, MU	La Murta	Terrace	Calmel-Avila (2002)	^{14}C	0.55	0.08	
5	Librilla, MU	Algeciras	Terrace	Calmel-Avila (2002)	^{14}C	0.65	0.05	
6	Librilla, MU	Morotola	Terrace	Calmel-Avila (2002)	^{14}C	0.72	0.04	500 – 1000
7	Fte. Librilla, MU	Algeciras	Terrace	Calmel-Avila (2002)	^{14}C	0.80	0.04	
8	Fte. Librilla, MU	Algeciras	Terrace	Calmel-Avila (2002)	^{14}C	0.88	0.06	
9	Lorca, MU	La Hoya	Fan	Silva <i>et al.</i> (2008)	^{14}C	1.08	0.04	
10	Totana, MU	Río (Guad)	Lacustrine	Insua <i>et al.</i> (2015)	^{14}C	1.19	0.03	1000 – 1500
11	Totana, MU	Río (Guad)	Lacustrine	Insua <i>et al.</i> (2015)	^{14}C	1.25	0.03	
12	Huércal, AL	Ruchete	Fan	Masana <i>et al.</i> (2005)	^{14}C	1.31	0.04	
13	Lorca, MU	Colmenar	Fan	Martínez Díaz <i>et al.</i> (2003)	^{14}C	1.35	0.04	
14	Albox, AL	Ruchete	Fan	Masana <i>et al.</i> (2005)	TL	1.45	0.04	
15	Totana, MU	Karting	Fan (d)	Roquero <i>et al.</i> (2019)	OSL	1.70	0.10	1500 – 2000
16	Totana, MU	Acopios 1	Lacustrine	Insua <i>et al.</i> (2015)	^{14}C	1.79	0.03	
17	Totana, MU	Alcanara	Fan (d)	Silva <i>et al.</i> (2008)	^{14}C	1.89	0.04	
18	Totana, MU	Alcanara	Fan (d)	Silva <i>et al.</i> (2008)	^{14}C	1.90	0.03	
19	Totana, MU	Río (Guad)	Lacustrine	Insua <i>et al.</i> (2015)	^{14}C	2.00	0.03	
20	Totana, MU	Acopios 2	Lacustrine	Insua <i>et al.</i> (2015)	^{14}C	2.21	0.03	
21	Totana, MU	Acopios 1	Lacustrine	Insua <i>et al.</i> (2015)	^{14}C	2.30	0.03	2500 – 3000
22	Librilla, MU	Librilla	Fan (d)	Calmel-Avila (2002)	^{14}C	2.39	0.05	
23	Totana, MU	Acopios 2	Lacustrine	Insua <i>et al.</i> (2015)	^{14}C	2.42	0.03	
24	Librilla, MU	Librilla	Fan	Calmel-Avila (2002)	^{14}C	2.51	0.05	
25	Totana, MU	Río (Guad)	Lacustrine	Insua <i>et al.</i> (2015)	^{14}C	2.53	0.03	
26	Totana, MU	Karting	Fan (d)	Roquero <i>et al.</i> (2019)	OSL	2.60	0.40	
27	Totana, MU	Acopios 1	Lacustrine	Insua <i>et al.</i> (2015)	^{14}C	2.65	0.03	
28	Totana, MU	Alcanara	Fan (d)	Silva <i>et al.</i> (2008)	^{14}C	2.72	0.04	2500 – 3000
29	Lorca, MU	Colmenar	Fan	Martínez Díaz <i>et al.</i> (2003)	^{14}C	2.85	0.07	
30	Lorca, MU	Lorca City	Fan	Silva <i>et al.</i> (2008)	^{14}C	3.37	0.04	
31	Lorca, MU	Colmenar	Fan	Martínez Díaz <i>et al.</i> (2003)	^{14}C	3.39	0.04	3500 – 3000
32	Goñar, AL	Huercal	Fan	Ortuño <i>et al.</i> (2012)	OSL	3.57	0.30	
33	Lorca, MU	Lorca City	Fan	Strydonck <i>et al.</i> (1995)	^{14}C	3.49	0.03	
34	Totana, MU	Río (Guad)	Lacustrine	Insua <i>et al.</i> (2015)	^{14}C	3.58	0.03	4000 – 3500
35	Lorca, MU	Colmenar	Fan	Martínez Díaz <i>et al.</i> (2003)	^{14}C	3.66	0.03	
36	Librilla, MU	Librilla	Fan (d)	Calmel-Avila (2002)	^{14}C	3.88	0.06	

Table 4b. Details on available published ages of Late Holocene alluvial deposits (OIS1) provided by several authors in the semi-arid SE Spain (Almería and Murcia region) using different dating methods: Radiocarbon (^{14}C); Quartz Thermoluminescence (TL); Quartz optically stimulated luminescence (OSL).

Tabla 4b (continuación). Detalles sobre las edades publicadas para depósitos aluviales del Holoceno reciente proporcionadas por diferentes autores para el SE semiárido de España (regiones de Murcia y Almería) mediante su datación por diferentes métodos: Carbono catorce (^{14}C); Termoluminiscencia convencional (TL); Termoluminiscencia ópticamente estimulada (OSL).

Rank	Zone	Site	Landform	Authors (year)	Dating Method	Age	Error ±	bin
37	Totana, MU	Río (Guad)	Lacustrine	Insua <i>et al.</i> (2015)	^{14}C	4.06	0.03	
38	Librilla, MU	Librilla	Fan (d)	Calmel-Avila (2002)	^{14}C	4.31	0.06	4500 - 4000
39	Librilla, MU	Librilla	Fan (d)	Calmel-Avila (2002)	^{14}C	4.50	0.10	
40	Librilla, MU	Librilla	Fan (d)	Calmel-Avila (2002)	^{14}C	4.50	0.04	
41	Librilla, MU	Librilla	Fan (d)	Calmel-Avila (2002)	^{14}C	4.61	0.15	500 - 4500
42	Lorca, MU	Lorca City	Fan	Strydonck <i>et al.</i> (1995)	^{14}C	4.62	0.04	
43	Librilla, MU	Librilla	Fan (d)	Calmel-Avila (2002)	^{14}C	5.61	0.33	
44	Librilla, MU	El Romeral	Fan (d)	Calmel-Avila (2002)	^{14}C	6.34	0.60	
45	Lorca, MU	Colmenar	Fan	Martínez Díaz <i>et al.</i> (2003)	^{14}C	6.35	0.04	6500 - 6000
46	Totana, MU	Río (Guad)	Lacustrine	Insua <i>et al.</i> (2015)	^{14}C	6.38	0.04	
47	Lorca, MU	La Hoya	Fan	Silva <i>et al.</i> , (2008)	^{14}C	6.69	0.50	6500 - 7000
48	Lorca, MU	La Hoya	Fan	Silva <i>et al.</i> , (2008)	^{14}C	6.69	0.04	
49	Lorca, MU	La Hoya	Fan	Silva <i>et al.</i> , (2008)	^{14}C	7.07	0.05	
50	Totana, MU	Acopios 2	Lacustrine	Insua <i>et al.</i> (2015)	^{14}C	7.98	0.04	
51	Huércal, AL	Ruchete	Fan	Masana <i>et al.</i> (2005)	TL	8.20	0.78	8500 - 8000
52	Lorca, MU	Comenar	Fan	Martínez Díaz <i>et al.</i> (2003)	^{14}C	8.22	0.05	
53	Totana, MU	Karting	Fan (d)	Roquero <i>et al.</i> (2019)	OSL	9.90	0.50	
54	Totana, MU	Río (Guad)	Lacustrine	Insua <i>et al.</i> (2015)	^{14}C	10.02	0.05	10,500 - 10,000
55	Totana, MU	Acopios 2	Lacustrine	Insua <i>et al.</i> (2015)	^{14}C	10.24	0.04	
56	Totana, MU	Río (Guad)	Lacustrine	Insua <i>et al.</i> (2015)	^{14}C	11.05	0.05	
57	Huércal, AL	Ruchete	Fan	Masana <i>et al.</i> (2005)	TL	11.10	0.92	11,500 - 11,000
58	Totana, MU	Acopios 2	Lacustrine	Insua <i>et al.</i> (2015)	^{14}C	11.46	0.05	

itself and the maximum and minimum ages covered by its associated uncertainty (three ages: value = 3). Since most of the data are derived from radiocarbon dating with associated uncertainty of 2σ , lower or equal to 0.05 ka (50 years), the individual scores hardly overlap two 500 years' time-bins (Tables 4a and 4b). For instance, a bin that contains the minimum, mean and maximum ages of a date is scored with a value of three (3). In the case

that the bin only holds the minimum and the mean age it is scored with a value of 2 and the subsequent bin holding the maximum age will have only a score of 1. In this way, a bin scored with 3 overlapped by uncertainties (value =1) of other age-data would receive a score of 4, 5, 6, etc. depending on the number of age-data overlapping the bin. Consequently, the resulting frequency distribution will display peaks or troughs (maximum and mini-

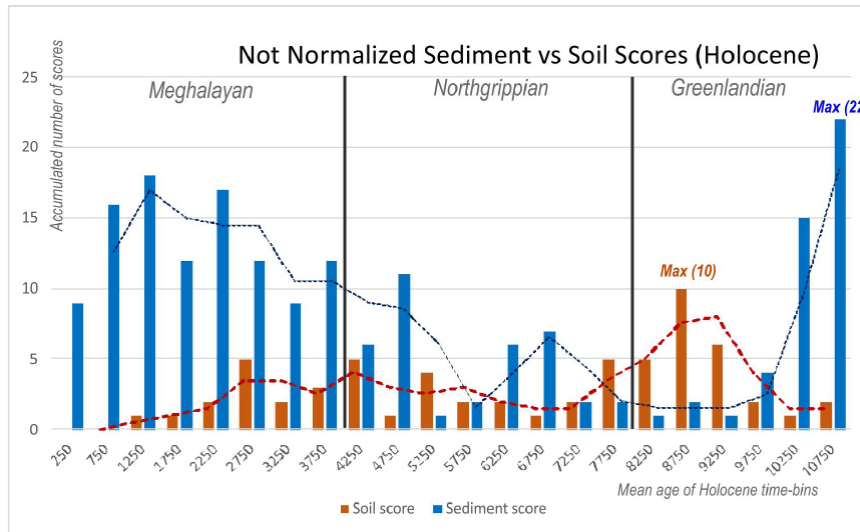


Figure 4. Histogram displaying not-normalized sediment and soil scores in time-bins of 500 years for the Holocene resulting for the application of age score counting explained in text. Second period mean-mobile curves are displayed for each data set.

Figura 4. Histogramas correspondientes a los valores no-normalizados de los scores de sedimentos y suelos en intervalos (time-bins) de 500 años para el Periodo Holoceno, resultantes del método de contejo de edades explicado en el texto. Las curvas de las medias-móviles de segundo periodo para ambos conjuntos de datos también se muestran en el gráfico.

mum) indicating main periods of sedimentation or soil development. Figure 4 displays the obtained scores for soils and sediments for each of the considered time-bins for the Holocene period. As in the case of the Pleistocene dataset (section 3.1), due to the important misbalance between the number of age-data for soils (15) and sediments (60), the values have been normalized for its representation in a frequency distribution curve (Fig. 5).

4. Results and discussion

In this section Pleistocene and Holocene age records and resulting respective age frequency curves will be presented and discussed separately according to the different nature and amount of age accounts for both periods (Tables 1 to 4).

4.1. The Pleistocene records

The age distribution for the last c. 700 ka displayed in figure 3 suggests that pedogenic

processes leading the formation of calcrete horizons and calcic soils in SE Spain primarily occurs during warm isotope stages from OIS 9 to OIS1, with very few calcrete ages occurring during cold glacial/stadial stages (OIS 8 to 2). Despite the modest amount of age data, from 300 to 150 ka calcrete development and sediment production display a clear alternating pattern of peaks of calcrete scores coinciding with troughs of sediment ones and vice-versa (Fig. 3). Due to the major amount of data for the last 150 ka, normalized age-frequency curves exponentially grow and overlap in this period. However, the pattern of peaks of calcrete scores coinciding with throughs of sediments are visibly enhanced during the entire last interglacial period (OIS 5), especially during the stadials 5a and 5c. In contrast, the warm stadial of the OIS3 displays a large anomaly with a significant drop in both sediment production and soil formation between c. 60 and 30 ka, labelled in the age frequency curves of figure 3 as the “OIS 3 anomaly”.

Calcrete/soil development seems to be a function of the environments that exist-

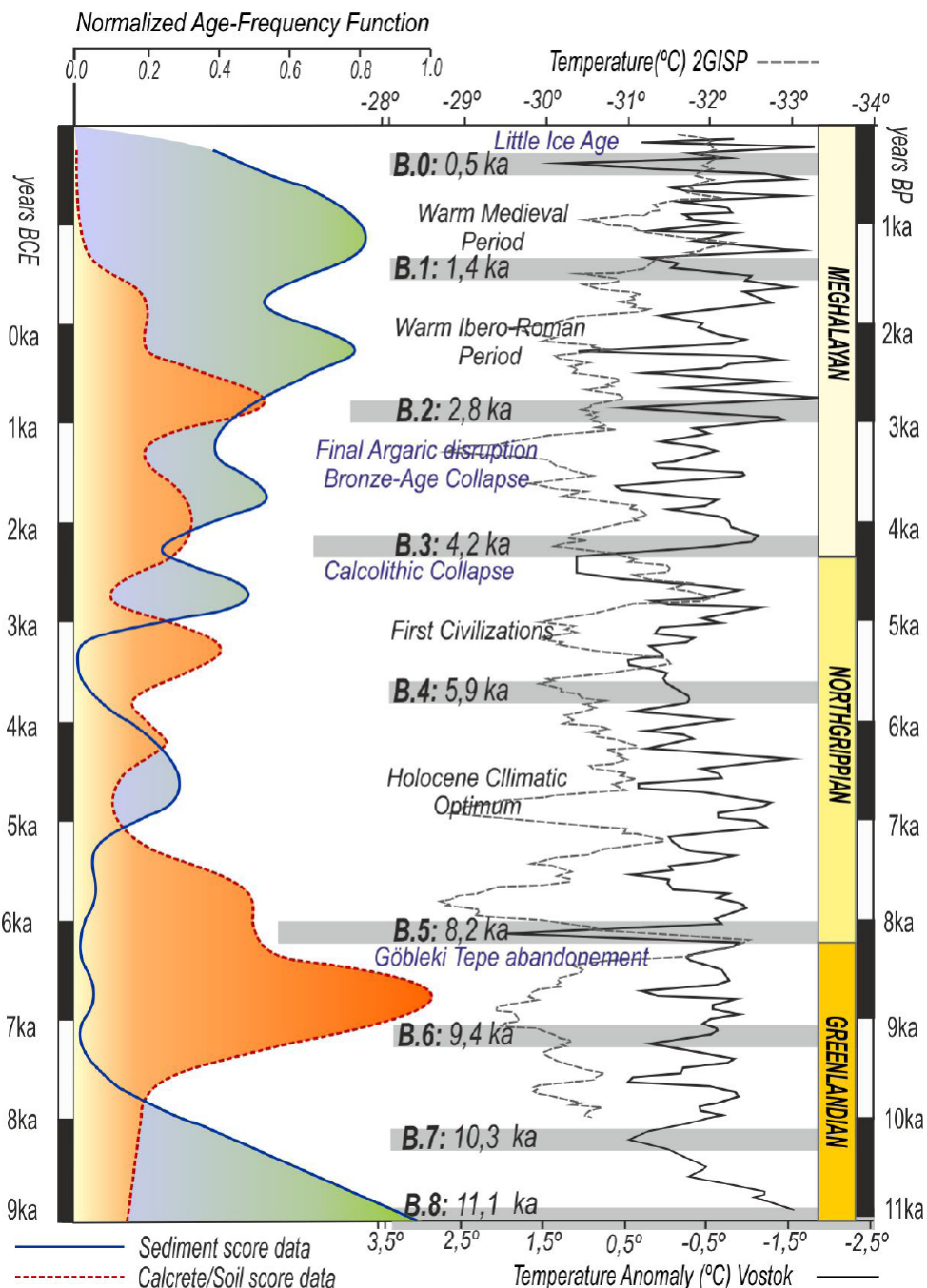


Figure 5. Normalized frequency distribution curve for sediment (solid line) and soil calcrite (dotted line) scores calculated in this study for SE Spain. Maximum sediment score before normalization was 28 in bin 10.5-11 ka. Maximum soil score was 22 in bin 8.5-9.0 ka. Climatic framework modified from Silva et al. (2017). B.1, B.2, etc. denote Bond Events.

Figura 5. Curva de distribución de frecuencias normalizadas para los scores acumulados de sedimentos (línea continua) y suelos carbonatados (línea discontinua) calculadas en este estudio para el SE de España. El score máximo de sedimento antes de la normalización era de n= 28 en el bin 10,5-11,0 ka. El score máximo del para suelos era de n=22 en el bin 8,5-9,0 ka. Marco climático modificado a partir de Silva et al. (2017). B.1, B.2, etc., indican los Eventos Bond.

ed during warm isotope stages in SE Spain, which favoured pedogenetic processes of carbonate leaching and accumulation. These favourable conditions are enhanced during the last phases of these warm isotope stages, as visibly occur during OIS1, OIS5 and OIS9 (Fig. 3). As proposed by previous authors (i.e. Candy and Black, 2009; Roquero *et al.*, 2019) in semiarid regions it is likely that increased aridity during the intervening glacial stages, coupled with reduced vegetation and accelerated landscape instability, was crucial in reducing rates of calcrete formation. The “OIS 3 anomaly” occurred during the last glacial cycle and aridity, from the hydric point of view, would be extreme as it can be deduced by the overlapped sediment and soil minimums on the respective age frequency curves (Fig. 3). There was not enough water for sediment production neither for the activation of pedogenic processes. Maybe enhanced erosion and large-scale landscape instability dominated this period (c. 60 to 30 ka), during which the last Neanderthal populations become eventually extinct in south Spain. In the case of the present interglacial, soil formation dominated during its first 5000 years, after a period of significant sedimentation between 15,000 and 10,000 years largely related with the deglaciation (Fig. 3). Detailed data on the Holocene period will be analysed in section 4.2.

On the other hand, sediment production primarily occurs during the intervening cold periods, but especially during the glacial-interglacial transitions and initial phases of warm stages. This is especially visible during the so-called Terminations I, II and III (deglaciations), related to the end of the cold isotope stages OIS2, OIS6 and OIS 8 respectively (Fig. 3). Among these Pleistocene cold periods, the OIS 6 represents a probable anomaly, since during the first half of this cold stage (c. 180 – 150 ka) soil development dominates displaying a discrete peak in the graphic of figure 3. This anomaly could be related with some findings in the eastern Mediterranean indicating the occurrence of very low negative values of $\delta^{18}\text{O}$ (-6‰ to -12‰) and $\delta^{13}\text{C}$ (-11‰)

typical of warm intervals during the period c.178 to 152 ka (Ayalon *et al.*, 2002). These authors indicate that rainfall increased dramatically due to the northwards shift of the African monsoons, but the isotopic records indicate that climate was as cold as much of the last glacial, but the conditions were never as dry. In the graphic of figure 3 this period has been labelled as the “OIS 6 Ayalon02 Anomaly” and the corresponding curve of anomalous $\delta^{18}\text{O}$ values recorded by Ayalon *et al.* (2002) is plotted in dotted line. Paleoecological data from Spain indicate that precipitation was sufficient in southern Mediterranean Europe during OIS 6 for the persistence of temperate vegetation areas (Blain *et al.*, 2017). Detailed herpetofaunal data for the southern Spanish meseta indicate the persistence of a Mediterranean-like climate during the early OIS 6, with subhumid rainfall values of c. 580 ± 40 mm /year sustaining open grasslands and woodlands areas in a 35% of the landscape (Blain *et al.*, 2019) favourable for soil development.

The older identified peak of calcrete development is related to the last phases of the warm isotopic stage OIS9, around 300 ka (Candy and Black, 2009; Roquero *et al.*, 2019). During this period, mature calcretes topping the oldest preserved fan surfaces in SE Spain developed (Silva 2015). Fluvial terraces of this age and older ones also show the development of similar mature calcretes (Candy and Black, 2009), which could be up to 2-3 m thick, with nice laminar horizons (Alonso-Zarza *et al.*, 1998). This phase of sedimentation, ending at c. 300 ka, marks the end of the most relevant phase of uplift along the faulted mountain front of the zone (relief generation) and coincides with the second phase of alluvial fan development of Silva (2015). The alluvial fan sediments of the first phase are tectonised and incorporated to the marginal reliefs. From this period on, tectonic modification of the relief is very limited, restricted to relatively small surface faulting events of metric scale (Silva 2015), and climate takes the control in fan sedimentation (Fig. 2). In this way, the older Quaternary soils be-

longing to the first phase, are not exposed at the ground surface, but preserved in the sedimentary sequences of the area. These normally outcrop as successions of seven to eight variably developed red paleosols (Fig. 3) occurred during the Brunhes Normal Chron (Somoza *et al.*, 1988). Using the paleoclimatic analogues for soil sequences proposed for the zone (Roquero *et al.*, 2019) is possible to infer periods of soil development up to the latest stages of OIS 17 around 700-710 ka (Fig. 3). These data imply that the second phase of fan sedimentation of Silva *et al.* (1992) would start around the isotopic stage OIS 17, soon after the Middle-Lower Pleistocene boundary at 780 ka. Data from Roquero *et al.* (2019) indicate that carbonate accumulation and re-carbonation of previous red soils (Bt horizons) developed in the zone, starts to be significant from the isotope stage OIS 11, which presents similar environmental conditions to OIS 1 in the Mediterranean region (Ayalon *et al.*, 2002). However, from OIS 9 onwards widespread calcrete development dominated (Fig. 3). Less mature calcretes occur during the OIS 5 and calcic soils (calcic horizons) developed during the early Holocene, which show larger peaks in the age frequency curve due to the larger amount of geochronological data for that periods (Fig. 3).

4.2. The Holocene records

The age distribution for the last c. 11,000 years displayed in figure 4 also shows alternating periods of soil formation and sediment production during Holocene and historic times. The analysis, clearly identify the climatic events of 8.2 and 4.2 ka BP, recently considered GSSP for the base of Northgriplian and Megalayan respectively (Walker *et al.*, 2018), as drier periods where minor sedimentation but enhanced soil formation took place, especially during the first event, which records the maximum score for soil formation processes (Fig. 4).

The obtained frequency age curves clearly display an overlapping and alternating pattern

of sediment production vs soil development from c. 11 to c. 4 ka, throughout the two first stages (Northgriplian and Greenlandian) of the Holocene (Fig. 4). During this initial time-span of the Holocene peaks (maximums) of sedimentation clearly coincides with troughs (minimums) of soil formation. Sedimentation reaches its maximum value during the end of the deglaciation between c. 11 and 10.5 ka, whilst soil formation reaches its maximum in the following timespan between 9.5 and 7.0 ka (Fig. 4). Is along this last time span, when sediment production reaches its lowest values of the entire Holocene, with minimum score (value = 1) during the Bond events B6 and especially B5 at 8.2 ka (Fig. 5). The latter is one of the driest periods of the Holocene being the boundary between the Northgriplian and the Greenlandian stages at global scale (Walker *et al.*, 2018). This boundary is highlighted by the analysis performed in this work, as the most important period of soil/calcrete development in SE Spain during the Holocene and, consequently, of landscape stabilization. The analysis also identifies the Holocene optimum (c. 6 ka), as well as the historical Roman and Medieval warm periods as phases of major sedimentation (Fig. 5).

The alternating patter of sediment and soil development frequency curves continues after 7 ka and sediment production is recovered during the Holocene Climatic Optimum, but with score values about 70 - 60% lower than those recorded during the first period (Figs. 4 and 5). Sedimentation peaks are also clearly related to other Holocene warm periods, showing increasing values. This is the case of those linked to the dawn of the first civilizations (c. 5 ka), the Early Bronze Age (c. 3.5 ka), the Roman and the Medieval warm periods (Fig. 5). During this second period of the Holocene increasing sedimentation occurs, but significant peaks of soil development are almost coincident or immediately occurred soon after the Bond events B4, B3 and B2 (Fig. 5).

Although it is not the most relevant peak, that related to the B3 Event fairly coincides with Northgriplian and Meghalayan bound-

ary at 4.2 ka. In many middle to low latitude regions, this transition coincides with an abrupt aridification period at 4.2 ka, having in some areas profound societal effects, with rain-fed region abandonments and societal collapses archaeologically visible across the eastern Mediterranean (Greece, Palestine, Egypt), Mesopotamia, the Indus Valley and also in Spain (Walker *et al.*, 2019). In detail, the 4.2 ka event in SE Spain coincides with the abrupt end of the Calcolithic settlements of Los Millares culture (Almería) and their sharp replacement by the Argaric culture of the early Bronze Age as displayed by “*summed calibrated radiocarbon date range distributions*” (SCRDRDs) for archaeological sites in SE Spain (Blanco-Gonzalez *et al.*, 2018). In this sense, well developed Calcolithic soil horizons dated to 4400 to 4200 cal. yr BP are prominent features across the Guadalentín Depression (Murcia) topping pre-Meghalayan sequences of palustrine deposits (Calmel-Avila, 2002). This chalcolithic soil coincides with a period of fan surface stabilization (no deposition), the initial stages of fluvial dissection in (Silva *et al.*, 2008) and a sharp population drop in the whole area (Calmel-Avila, 2002).

The last peak of soil development occurred closely related to the Bond Event B2 (2.8 ka BP). This event is not globally significant, but relevant in the semiarid SE Spain. It is linked to the eventual collapse of the Argaric Bronze Age societies in the area, including the settlement of La Bastida de Totana, the largest megapolis in Europe during this Period (Blanco-Gonzalez *et al.*, 2018), and the general desiccation and dissection of the palustrine environments in the Murcia region (Silva *et al.*, 2008). This episode of soil development is characterized by the recarbonation of organic soils and sediments deposited during the early Bronze Age (Roquero *et al.*, 2019b) and an important depopulation of the zone, which is not recovered again until Ibero-Roman times (2.2 - 2.0 ka BP; Calmel-Avila, 2002; Blanco-Gonzalez *et al.*, 2018). From this episode on, no significant soil development are recorded by the available geochronological data and major sedimentary inputs are linked to

both the Warm Roman and Medieval periods (Fig. 4). During the Little Ice Age, sedimentation is related both to terrace development in entrenched fan surfaces and into dissected palustrine wetlands (Silva *et al.*, 2008). These two events at 4.2 ka BP (B3), but specially that at 2.8 ka BP (B2) were of special significance in SE Spain promoting the onset of erosive geomorphological processes leading to the development of the fluvial incision, wetland desiccation triggering the present arid landscapes in the whole area.

5. Conclusions

The present study gathers 168 dates, 52 for calcic soils and calcretes and 116 for sediments, covering the last 400 ka. The analysis is based in the construction of age-frequency distribution functions which have been partitioned in two sets of age-data. The first dataset considers the last 400 ka (excluding the last 5 ka) and the second one for the last 11,000 years (i.e. the Holocene period). The age-frequency distribution functions are based on that developed by Candy and Black (2009) for the analysis of periods of calcrete development in SE Spain. To construct the Pleistocene age-frequency curves (Fig. 3) the last 400 ka were subdivided in time-periods (bins) of 5 ka, which offer enough resolution to distinguish among the different Oxygen Isotopic stages (OIS) occurred during the period of analysis. This first analysis excludes age-data for the last 5ka, since the big amount of age records published for this time-period would produce an anomalous peak in the resulting curves. To construct the Holocene age-frequency curves (Fig. 5) more numerous and detailed radiocarbon age-estimations were used differentiating smaller time-periods (bins) of only 500 years (0.5 ka).

The study identifies alternating periods of sedimentation and soil formation since the Brunhes-Matuyama boundary (OIS 17 – OIS 18). Calcretes and calcic soils appear as elements developed during the last phases of warm isotopic stages, whilst sedimentation

dominated during the transition between warm-cold isotopic stages, especially during terminations III to I, coinciding with deglaciation periods (Fig. 3). Soil and calcrete formation display peaks of enhanced development in the warm isotopic stages OIS 9, OIS 5 and OIS 1. The two first periods corresponds to the termination of the first and second phases of alluvial fan development in SE Spain. The OIS 1 calcrete-period is restricted to the early Holocene (Greenlandian stage) and culminates the third phase of alluvial fan development (Fig. 2). Subsequent phases of sedimentation correspond to different prehistorical and historical periods linked to Bond Events (Fig. 5).

Climatic anomalies detected in isotope stages OIS 3 (warm) and OIS 6 (cold) can be related to regional anomalies in the Mediterranean region linked to anomalous shifts of the African Monsoons (Ayalon *et al.*, 2002). It is to note that the OIS 3 anomaly points to very dry (hydric) conditions, displaying severe minimum values in both sedimentation and soil scores in the obtained age-frequency curves (Fig. 3). In other words, a period with insufficient available water for sediment production (runoff), but also for soil formation (infiltration) and presumably dominated by erosion, desertification and rapid landscape change in SE Spain. These severe dry climatic conditions coincide with the period (c. 60 – 30 ka BP) of extinction of the last Neanderthal populations in South Spain.

The age-frequency function for the Holocene (c. last 11,000 years BP) clearly discriminates the climatic events of 8.2 and 4.2 ka as drier periods with minor sedimentation values. The Holocene starts with a sharp period of sedimentation linked to the last stages of the deglaciation after the “younger Dryas”. This sedimentary period is followed by a longer arid and dry phase until c. 8.2 ka in which sedimentation decreased dominating soil formation (i.e. fan surface encrustment). After this event, sedimentation re-start dominated by a limited distal offlap aggradation towards basin centre locations. This renewed sedimentation, shows a near-cyclic pattern with sedi-

ment maximums during the different climatic optimums of the Holocene controlled by Bond events. Of special interest is the record of the 4.2 and 2.4 ka BP events as arid periods dominated by soil formation and recarbonation processes, also linked to the collapse of Los Millares chalcolithic and the Argaric Late Bronze populations in SE Spain (i.e. Calmel Avila, 2002; Blanco-Sánchez *et al.*, 2018). These two last events point to the onset of the present arid environments, generalized fluvial dissection and torrential behaviour of the fluvial systems in SE Spain.

Eventually it is noteworthy to point out that the set of ages used in this study come from very different studies, with different objectives. However, the obtained age frequency distribution curves depict not only the most important climatic fluctuations occurred during the Pleistocene, but also during the antiquity, identifying the 2.4, 4.2 and 8.2 ka BP climatic events as dry periods prompt to develop calcic soils introducing severe geomorphological changes in the zone.

Acknowledgements

The authors are grateful to the reviews of Dr. Álvaro Rodríguez Berriguete and an anonymous referee. The MINECO-FEDER Research Project CGL2015-67169-P (QTECTSPAIN – USAL) has funded this work.

References

- Alonso Zarza, A.M.; Silva, P.G.; Goy, J.L.; Zazo, C. (1998). Fan-surface dynamics, plant-activity and calcrete development: Interactions during ultimate phases of fan evolution in the semiarid SE Spain (Murcia). *Geomorphology*, 24, 147-167. [https://doi.org/10.1016/S0169-555X\(98\)00022-1](https://doi.org/10.1016/S0169-555X(98)00022-1)
- Ayalon, A.; Bar-Matthews, M.; Kaufman, A. (2002). Climatic conditions during marine oxygen isotope stage 6 in the eastern Mediterranean region from the isotopic composition of speleothems of Soreq Cave, Israel. *Geology*, 30 (4), 303-306. [http://dx.doi.org/10.1130/0091-7613\(2002\)030<0303:CCDMOI>2.0.CO;2](http://dx.doi.org/10.1130/0091-7613(2002)030<0303:CCDMOI>2.0.CO;2)

- Blain, H.A.; Cruz Silva, J.A.; Jiménez Arenas, J.M.; Margari, V.; Roucoux, K. (2018). Towards a Middle Pleistocene terrestrial climate reconstruction based on herpetofaunal assemblages from the Iberian Peninsula. *Quaternary Science Reviews*, 191, 167-188. <https://doi.org/10.1016/j.quascirev.2018.04.019>
- Blain, H.A.; Bisbal-Chinesta, J.F.; Martínez-Monzón, A.; Panera, J.; Rubio-Jara, S.; Uribelarrea, D.; Yravedra, J.; Pérez-González, A. (2019). The Middle to Late Pleistocene herpetofaunal assemblages from the Jarama and Manzanares valleys (Madrid, central Spain): An ecological synthesis. *Quaternary International*, 520, 49-63. <https://doi.org/10.1016/j.quaint.2018.03.004>
- Blanco-González, A.; Lillios, K. T.; López-Sáez, J.A.; Drake, B. L. (2018). Cultural, Demographic and Environmental Dynamics of the Copper and Early Bronze Age in Iberia (3300-1500 BC): Towards an Interregional Comparison at the Time of the 4.2 ky BP Event. *Journal of World Prehistory*, 31, 1-79. <https://doi.org/10.1007/s10963-018-9113-3>
- Calmel-Avila, M. (2002). The Librilla "rambla" an example of morphogenetic crisis in the Holocene (Murcia, SE Spain). *Quaternary International*, 93-94, 101-108. [https://doi.org/10.1016/S1040-6182\(02\)00009-5](https://doi.org/10.1016/S1040-6182(02)00009-5)
- Candy, I.; Black, S. (2009). The timing of Quaternary calcrete development in semi-arid southeast Spain: Investigating the role of climate on calcrete genesis. *Sedimentary Geol.*, 218, 6-15. <https://doi.org/10.1016/j.sedgeo.2009.03.005>
- Delgado Castilla, L. (2009). Edades U/Th de los tránsitos del cuaternario reciente de la Cuenca de Tabernas, Almería: implicaciones en su evolución geodinámica y paleoambiental. *Cuaternario y Geomorfología*. [http://tierra.rediris.es/CuaternarioyGeomorfologia/images/vol23_1_2/Cuater%2023\(1-2\)_\(04\)Delgado.pdf](http://tierra.rediris.es/CuaternarioyGeomorfologia/images/vol23_1_2/Cuater%2023(1-2)_(04)Delgado.pdf)
- Ferrater, M.; Ortúñoz, M.; Masana, E.; Martínez-Díaz, J.J.; Pallàs, R.; Perea, H.; Baize, S.; García-Meléndez, E.; Echeverría, A.; Rockwell, T.; Sharp, W.D.; Arrowsmith, R. (2017). Lateral slip rate of Alhama de Murcia fault (SE Iberian Peninsula) based on a morphotectonic analysis. *Quaternary International*, 451, 87-100. <http://dx.doi.org/10.1016/j.quaint.2017.02.018>
- García-Meléndez, E.; Goy, J.L.; Zazo, C. (2003). Neotectonics and Plio-Quaternary landscape development within the eastern Huercal-Overa Basin (Betic Cordilleras, southeastern Spain). *Geomorphology*, 50, 111-133. [https://doi.org/10.1016/S0169-555X\(02\)00210-6](https://doi.org/10.1016/S0169-555X(02)00210-6)
- Goy, J.L.; Zazo, C. (1986). Synthesis of the Quaternary in the Almería littoral neotectonic activity and its morphological features, western Betics, Spain. *Tectonophysics*, 130, 259-270. [https://doi.org/10.1016/0040-1951\(89\)90259-X](https://doi.org/10.1016/0040-1951(89)90259-X)
- Harvey, A.M.; Miller, S.Y.; Wells, S.G. (1995). Quaternary soil and river terrace sequences in the Aguas / Feos river systems: Sorbas basin, southeast Spain. In: *Mediterranean Quaternary River Environments* (J. Lewin; M.G. Macklin; J.C. Woodward, eds.). Balkema, Rotterdam.
- Harvey, A.M.; Whitfield, E. (nee Maher); Stokes, M.; Mather, A.E. (2014). The Late Neogene to Quaternary Drainage Evolution of the Uplifted Neogene Sedimentary Basins of Almería, Betic Chain. In: *Landscapes and landforms of Spain* (F. Gutiérrez; M. Gutiérrez, eds.). World Geomorphological Landscapes Series. Springer, Dordrecht, 37-62. https://doi.org/10.1007/978-94-017-8628-7_3
- Illiott, S.H. (2014). *Cosmogenic dating of fluvial terraces in the Sorbas basin, SE Spain*. Ph.D. Thesis. University of Plymouth, UK. 345 pp.
- Insua, J.M.; García-Mayordomo, J.; Salazar, A.; Rodríguez-Escudero, E.; Martín-Banda, R.; Álvarez-Gómez, J.A.; Canora; C.; Martínez-Díaz, J.J. (2015). Paleoseismological evidence of Holocene activity of the Los Tollos Fault (Murcia, SE Spain): A lately formed Quaternary tectonic feature of the Eastern Betic Shear Zone. *Journal of Iberian Geology*, 41 (3), 333-350. http://dx.doi.org/10.5209/rev_JIGE.2015.v41.n3.49948
- Lewin, J.; Macklin, M.G.; Woodward, J.C. (1995). *Mediterranean Quaternary River Environments*. Balkema, Rotterdam. 287 pp.
- Macklin, M.G.; Fuller, I.C.; Lewin, J.; Maas, G.S.; Passmore, D.G.; Rose, J.; Woodward, J.C.; Black, S.; Hamlin, R.H.B.; Rowan, J.S. (2002). Correlation of fluvial sequences in the Mediterranean basin over the last 200 ka and their relationship to climate change. *Quaternary Science Reviews*, 21, 1633-1641. [https://doi.org/10.1016/S0277-3791\(01\)00147-0](https://doi.org/10.1016/S0277-3791(01)00147-0)
- Martínez-Díaz, J.J.; Masana, E.; Hernández-Enrile, J.L.; Santanach, P. (2003). Effects of repeated paleo-earthquakes on the Alhama de Murcia fault (Betic Cordillera, Spain) on the Quaternary evolution of an alluvial fan system. *Annals of Geophysics*, 46 (5), 775-792. <https://doi.org/10.4401/ag-3455>

- Masana, E.; Martínez Díaz, J.J.; Hernández-Enrile, J.L.; Santanach, P. (2004). The Alhama de Murcia fault (SE Spain), a seismogenic fault in a diffuse plate boundary. *Journal of Geophysical Research*, 109, B01301: 1-17. <https://doi.org/10.1029/2002JB002359>
- Masana, E.; Pallàs, R.; Perea, H.; Ortúñoz, M.; Martínez-Díaz, J.J.; García-Meléndez, E.; Santanach, P. (2005). Large Holocene morphogenic earthquakes along the Albox fault, Betic Cordillera, Spain. *Journal of Geodynamics*, 40, 119-133. <https://doi.org/10.1016/j.jog.2005.07.002>
- Masana, E.; Moreno, X.; Gràcia, E.; Pallàs, R.; Ortúñoz, M.; López, R.; Gómez-Novell; Ruano, P.; Perea, H.; Štepancíková, P.; Khazaradze, G. (2018). First evidence of paleoearthquakes along the Carboneras Fault Zone (SE Iberian Peninsula): Los Trances site. *Geologica Acta*, 16 (4), 461-476. <https://doi.org/10.1344/geologicaacta2018.16.4.8>
- Montenat, Ch. (1981). Observations nouvelles sur les croûtes calcaires pléistocènes du Sud-Est de l'Espagne Province d'Alicante et de Murcia. *Géologie Méditerranéene*, 8 3, 137-15. <https://doi.org/10.3406/geolm.1981.1163>
- Ortúñoz, M.; Masana, E.; García-Meléndez, E.; Martínez-Díaz, J.J.; Canora, C.; Štepancíková, P.; Cunha, P.; Sohbati, R.; Buylaert, J.P.; Murray, A.S. (2012). Paleoseismic study of a slow-moving and silent fault termination: The Alhama de Murcia-Góñar system (Eastern Betics, Spain). *Geological Society of America Bulletin*, 124 (9/10), 1474-1494. <https://doi.org/10.1130/B30558.1>
- Roquero, E.; Silva, P.G.; Rodríguez-Pascua, M.A.; Bardají, T.; Élez, J.; Carrasco-García, P.; Giner-Robles, J.L. (2019a). Geomorphology and pedology of faulted fan surfaces and paleosols in the Palomares Fault Zone (Betic Cordillera, SE Spain). *Geomorphology*, 342, 196-209. <https://doi.org/10.1016/j.geomorph.2019.06.003>
- Roquero, E.; Silva, P.G.; Élez, J.; Rodríguez-Pascua, M.A.; Medialdea, A. (2019b). Registro edáfico de los cambios paleoambientales en la Depresión del Guadalentín durante el Holoceno (Murcia, SE España). En: Actas XV Reunión Nacional de Cuaternario AEQUA, Bilbao, 235-237.
- Schulte, L.; Julià, R.; Burjachs, F.; Hilgers, A. (2008). Middle Pleistocene to Holocene geochronology of the River Aguas terrace sequence (Iberian Peninsula). *Geomorphology*, 98, 13-33. <https://doi.org/10.1016/j.geomorph.2007.03.018>
- Silva, P.G. (2014). The Guadalentín Tectonic Depression, Betic Cordillera, Murcia. In: *Landscape and landforms of Spain* (F. Gutiérrez; M. Gutiérrez, eds.). World Geomorphological Landscapes Series. Springer, Dordrecht, 25 -35. http://dx.doi.org/10.1007/978-94-017-8628-7_2
- Silva, P.G., Harvey, A.M., Goy, J.L., Zazo, C. (1992). Geomorphology, depositional style and Morphometric relationships of Quaternary alluvial fans in the Guadalentín Depression (Murcia, SE Spain). *Z. F. Geomorphologie*, 36, 325-341.
- Silva, P.G.; Goy, J.L.; Zazo, C.; Bardají, T. (2003). Fault generated mountain fronts in southeast Spain: geomorphologic assessment of tectonic and seismic activity. *Geomorphology*, 50, 203-226. [https://doi.org/10.1016/S0169-555X\(02\)00215-5](https://doi.org/10.1016/S0169-555X(02)00215-5)
- Silva, P.G.; Bardají, T.; Calmel-Ávila, M.; Goy, J.L.; Zazo, C. (2008). Transition from alluvial to fluvial systems in the Guadalentín Depression (SE Spain) during the Holocene: Lorca Fan versus Guadalentín River. *Geomorphology*, 100, 140-153. <https://doi.org/10.1016/j.geomorph.2007.10.023>
- Silva, P.G.; Bardají, T.; Roquero, E.; Martínez-Graña, A.; Perucha, M. A.; Lario, J.; Giner Robles, J.L.; Rodríguez-Pascua, M.A.; Pérez-López, R.; Cabero, A.; Goy, J.L.; Zazo, C. (2015). Seismic palaeogeography of coastal zones in the Iberian Peninsula: Understanding ancient and historic earthquakes in Spain. *Cuaternario y Geomorfología*, 29, 31-56. <http://dx.doi.org/10.17735/cyg.v29i1-2.31012>
- Silva, P.G.; Roquero, E.; Bardají, T.; Baena-Presley, J.; Cearreta, A.; Rodríguez-Pascua, M.A.; Rosas, A.; Zazo, C.; Goy, J.L. (2017). El Periodo Cuaternario: La Historia Geológica de la Prehistoria. *Cuaternario y Geomorfología*, 31 (3-4), 113-154. <https://doi.org/10.17735/cyg.v31i3-4.55588>
- Sohbati, R.; Murray, A. S.; Buylaert, J.-P.; Ortúñoz, M.; Cunha, P. P.; Masana, E. (2012). Luminescence dating of Pleistocene alluvial sediments affected by the the Alhama de Murcia fault (eastern Betics, Spain): a comparison between OSL, IRSL, and post-IR IRSL ages. *Boreas*, 41 (2), 250-262. <https://doi.org/10.1111/j.1502-3885.2011.00230.x>
- Somoza, L.; Zazo, C.; Goy, J.L.; Mörner, N.A. (1989). Estudio geomorfológico de secuencias de abanicos aluviales cuaternarios (Alicante – Murcia, España). *Cuaternario y Geomorfología*, 3, 73-82. [http://tierra.rediris.es/CuaternarioyGeomorfologia/images/vol3/cuaternario3\(1-4\)_010-.pdf](http://tierra.rediris.es/CuaternarioyGeomorfologia/images/vol3/cuaternario3(1-4)_010-.pdf)

- Stokes, M. (2008). Plio-Pleistocene drainage development in an inverted sedimentary basin: Vera basin, Betic Cordillera, SE Spain. *Geomorphology*, 100, 193-211. <https://doi.org/10.1016/j.geomorph.2007.10.026>
- Stokes, M.; Mather, A.; Rodés, Á.; Kearsey, S.; Lewin, S. (2018). Anatomy, Age and Origin of an Intramontane Top Basin Surface (Sorbas Basin, Betic Cordillera, SE Spain). *Quaternary*, 1(2), 15p. <https://doi.org/10.3390/quat1020015>
- Walker, M.; Head, M.J.; Berkelhammer, M.; Björck, S.; Cheng, H.; Cwynar, L.; Fisher, D.; Gkinis, V.; Long, A.; Lowe, J.; Newnham, R.; Rasmussen, S.O.; Weiss, H. (2019). Formal ratification of the subdivision of the Holocene Series/Epoch (Quaternary System/Period). *Episodes*, 41 (4), 213-223. <https://doi.org/10.18814/epiiugs/2018/018016>
- Wenzens, E.; Wenzens, G. (1997). The influence of tectonics, sea-level fluctuations and river capture on the Quaternary morphogenesis of the semi-arid Pulpí Basin (southeast Spain). *Catena* 30, 283-293. [https://doi.org/10.1016/S0341-8162\(97\)00016-7](https://doi.org/10.1016/S0341-8162(97)00016-7)

Recibido el 8 de abril de 2020

Aceptado el 1 de junio de 2020

